

# The kinematic cosmic dipole beyond Ellis and Baldwin

Albert Bonnefous<sup>1,\*</sup>

Sorbonne Université, CNRS, Institut d’Astrophysique de Paris, 98bis Boulevard Arago, 75014 Paris, France

Received YY 20ZZ

## ABSTRACT

The cosmic dipole anomaly—currently detected at a significance exceeding  $5\sigma$  in several independent survey poses a significant challenge to the standard model of cosmology. The Ellis & Baldwin formula provides a theoretical link between the intrinsic dipole anisotropy in the sky distribution of extragalactic light sources and the observer’s velocity relative to the cosmic rest frame, under the assumptions that the sources follow a power-law luminosity function and exhibit power-law spectral energy distributions. In this work, we demonstrate that this relation can be generalized to arbitrary luminosity distributions and spectral profiles. We derive the corresponding expression for the effective spectral index and apply it to a sample of quasars observed in the W1 band of the CatWISE survey. We show that the anomalous cosmic dipole persists beyond the power-law assumption. These results provide a more general and robust framework to interpret measurements of the cosmic dipole in future large-scale surveys.

## 1. Introduction

In their 1984 article (Ellis & Baldwin 1984), Ellis & Baldwin pointed out that our motion with respect to the Cosmological Rest Frame (CRF) induces an intrinsic anisotropy in the observed sky distribution of any class of objects in the Universe. In other words, the Universe does not appear perfectly homogeneous and isotropic to us. In the specific case of radio sources, whose spectra and flux distributions can be well approximated by power laws, they proposed a method to infer our velocity in the CRF by measuring this anisotropy, more precisely the dipole in the number of sources per unit solid angle. They derived what we will hereafter refer to as the EB formula:

$$\mathcal{D}_{\text{kin}} = (2 + x(1 + \alpha))\beta, \quad (1)$$

where  $x$  and  $\alpha$  denote the power-law indices of the flux distribution and source spectra, respectively, and  $\beta$  is our velocity relative to the CRF, normalized by the speed of light  $c$ . Ellis & Baldwin argued that estimating  $\beta$  in this way should yield the same result as the velocity measured from the dipole of the Cosmic Microwave Background (CMB), provided the sources are sufficiently distant that intrinsic clustering anisotropies can be neglected, and lie entirely beyond our local bulk flow, in a Friedmann-Lemaître-Robertson-Walker (FLRW) Universe.

At the time, however, applying this test to observational data was not feasible, due to the absence of sufficiently large catalogs to obtain a robust signal-to-noise ratio in the dipole measurement. In 2021, robust result of about  $5\sigma$  in statistical significance, was obtained using CatWISE quasar data (Secrest et al. 2021), and in 2022 it was shown that NVSS radio galaxies yield a similar result (Secrest et al. 2022). Despite being uncorrelated and affected by distinct systematics, both datasets yielded inferred velocities significantly larger than the CMB expectation. Within the  $\Lambda$ CDM framework, no explanation has yet

been found: while the statistical significance has been questioned (Abghari et al. 2024), recent analyses affirm that the result persists with a more refined description of higher multipoles (von Hausegger et al. 2025).

These findings have renewed interest in the EB formalism and motivated efforts to extend its application to upcoming surveys such as Euclid (Euclid Collaboration et al. 2025), LSST (Rubin Observatory) (Ivezić et al. 2019), and SPHEREx (Crill et al. 2020). In particular, the expression for the kinematic dipole in number counts has been generalized to a tomographic dipole that incorporates redshift dependence in the source description (Maartens et al. 2018; Dalang & Bonvin 2022). It has also been shown that the original EB formula remains correct in the presence of source evolution (von Hausegger 2024), within the power-law framework of the original Ellis & Baldwin article. A more detailed review on this test and its use through the year is available in (Secrest et al. 2025).

In this letter, we first briefly review the formalism underlying the EB formula in Section 2. We then extend it in Section 3 to the general case of a source population without assuming any specific spectral profile or luminosity distribution, considering two distinct survey types: monochromatic (measuring the flux density, as is typical of radio surveys) and bolometric (the flux is integrated, typical of photometric surveys). Finally, in Section 4, we apply the resulting effective spectral index to quasars and compare it to the value obtained using the approach of (Secrest et al. 2021).

## 2. The Ellis & Baldwin formula

Consider a moving observer with respect to a rest frame, such as presented in Fig. 1. Any quantity  $a$  measured in the frame of the observer will be written  $a_o$ , whereas the same quantity in the rest frame will be  $a_r$ . Two different effects impact the observations, the relativistic aberrations, and the Doppler boosting.

\* albert.bonnefous@iap.fr

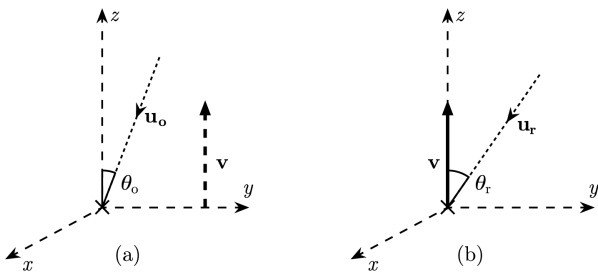


Fig. 1: (a) The frame moving with the observer, (b) the rest frame, in which the observer has a velocity  $\mathbf{v}$ . For the sake of simplicity, we assume that the  $z$  axis is parallel to the movement of this observer.

## 2.1. Relativistic aberration

The relativistic aberration of light is the *deformation* of the field of view of an observer moving with respect to what it observes; the apparent position of a body is shifted toward the direction of its movement. Suppose that we are looking at an object at a position  $\boldsymbol{\theta}_o = (\theta_o, \phi_o)$  in the sky. In the rest frame, the angle  $\phi_r$  does not change, and  $\theta_r$  transforms such that (Burles & Rappaport 2006):

$$\sin \theta_r = \frac{\sin \theta_o}{\gamma(1 - \beta \cos \theta_o)}, \quad (2)$$

where  $\gamma = 1/(1 - \beta^2)^{1/2}$ . With  $d\Omega = \sin \theta d\theta d\phi$ , we obtain the distortion of the solid angles relation:

$$d\Omega_o = \delta(\boldsymbol{\theta}_o)^{-2} d\Omega_r, \quad (3)$$

and introducing the notation:

$$\delta(\boldsymbol{\theta}) = \frac{1}{\gamma(1 - \beta \cdot \boldsymbol{\theta})} \approx 1 + \boldsymbol{\beta} \cdot \boldsymbol{\theta} + \mathcal{O}(\beta^2).$$

Also, for the sake of simplicity, the  $\mathcal{O}(\beta^2)$  will be omitted in every approximation that follows.

## 2.2. The relativistic Doppler effect

The Doppler boosting effects describes that the light coming from a distant object will be brighter, and bluer, in the direction of the movement of the observer. Between the two frames, the frequency of a given photon shifts as (Moriconi 2006):

$$\nu_o = \delta(\boldsymbol{\theta}_o) \nu_r. \quad (4)$$

The flux density of light  $S = \frac{dE}{d\nu dt}$  also transforms between frames as:

$$S_o(\nu_o) = \delta(\boldsymbol{\theta}_o) S_r(\nu_r). \quad (5)$$

## 2.3. Ellis & Baldwin formula with power laws

Up until now, the rest frame has been completely arbitrary. Now, let us assume that the rest frame is the CRF. If the observer had no movement with respect to this frame, they would observe a completely uniform background of objects  $N$ , this uniformity provided that they are *sufficiently far away* that local inhomogeneities can be negligible

(Gibelyou & Huterer 2012). These objects can be galaxies, quasars, *etc.*, but we will consider that there is only one type of object in our data. Ellis & Baldwin (Ellis & Baldwin 1984) make the following assumptions. First, every object's spectral flux density  $S$  has a simple power law dependence on the frequency  $\nu$ :

$$S \propto \nu^{-\alpha}. \quad (6)$$

Secondly, the sensitivity of our observational instrument is not infinite, therefore there is a limiting flux below which no objects can be detected. Now, if the objects have a power law distribution in the number of objects  $N$  above a certain flux  $S_{\lim}$ :

$$N(> S_{\lim}) \propto S_{\lim}^{-x}. \quad (7)$$

These two indices  $x$  and  $\alpha$  completely depend on the type of object we observe, their redshift distribution and the chosen flux cut. In the observer's frame, the flux received from one source is boosted by the Doppler effect, and using the power law (6), the flux received from this object at a fixed frequency  $\nu_o$  is:

$$S_o(\nu_o) = \delta(\boldsymbol{\theta}_o)^{1+\alpha} S_r(\nu_o). \quad (8)$$

The number of objects, in a given direction  $\boldsymbol{\theta}_o$ , then changes as:

$$\begin{aligned} dN_o(> S_{\lim}, \boldsymbol{\theta}_o) &= dN_r(> \delta(\boldsymbol{\theta}_o)^{-(1+\alpha)} S_{\lim}, \boldsymbol{\theta}_o) \\ &= \delta(\boldsymbol{\theta}_o)^{x(1+\alpha)} dN_r(> S_{\lim}, \boldsymbol{\theta}_o). \end{aligned} \quad (9)$$

Note that here,  $S_{\lim}$  is fixed and it is the objects' flux density that changes, which is *as if* the flux density limit depended on the frame. Finally, taking into account the aberration of the solid angles (3), the number count of objects by solid angle  $N_\Omega = \frac{dN}{d\Omega}$  in the observer frame becomes:

$$\begin{aligned} N_{\Omega,o}(> S_{\lim}, \boldsymbol{\theta}_o) &= \frac{dN_o}{d\Omega_o}(> S_{\lim}, \boldsymbol{\theta}_o) \\ &= \delta(\boldsymbol{\theta}_o)^{2+x(1+\alpha)} N_{\Omega,r}(> S_{\lim}). \end{aligned} \quad (10)$$

Since the rest frame is the cosmological rest frame, the number count of objects by solid angle is independent of direction  $N_{\Omega,r}(> S_{\lim}, \boldsymbol{\theta}_r) = \bar{N}_{\Omega,r}(> S_{\lim})$ . If we integrate this formula on the whole sky, the overall number of observed objects in the sky does not change with the frame, at least at order  $\beta$ , and we can write

$$\bar{N}_{\Omega,r}(> S_{\lim}) = \bar{N}_\Omega(> S_{\lim}) = N(> S_{\lim})/4\pi.$$

Note that if we want to take into account any other non-kinematic cosmological perturbation in the number count, we can do so by including them in this  $\bar{N}_\Omega$  (Nadolny et al. 2021).

Now, if we take the CMB as a reference frame, our speed relatively to this CRF is estimated to be  $v = 369.82 \pm 0.11 \text{ km.s}^{-1}$  (Collaboration et al. 2020). Therefore, we have  $\beta \ll 1$ , and the coefficient  $\delta(\boldsymbol{\theta}_o)$  can be approximated as  $\delta(\boldsymbol{\theta}_o) \approx 1 + \boldsymbol{\beta} \cdot \boldsymbol{\theta}_o$ . The number count (10) can be expressed purely with observed quantities, and we obtain

$$N_{\Omega,o}(> S_{\lim}, \boldsymbol{\theta}_o) \approx \bar{N}_\Omega(1 + \mathcal{D}_{\text{kin}} \cdot \boldsymbol{\theta}_o) \quad (11)$$

$$\mathcal{D}_{\text{kin}} = (2 + x(1 + \alpha))\boldsymbol{\beta} \quad (12)$$

This is the form derived by Ellis & Baldwin (Ellis & Baldwin 1984). We've seen that this expression assumes that the spectrum and luminosity function of these objects are power laws, and most of all that there exists a cosmological rest frame, in which there is a uniform background of these objects. However, since aberration and Doppler boosting are purely *local relativistic effects*, this formula is completely independent of the cosmological model provided that the cosmological principle holds. This formula also requires no knowledge of the redshift of the objects, only their location in the sky.

### 3. Kinematic dipole without any assumption on the spectrum and number count

Here, we want to derive a dipole expression, without making the power law hypothesis for the cumulative number count and spectrum of our sources. The assumptions we will make is that  $\beta \ll 1$  and that all of the sources that we are considering, have the same redshift, and have the same spectrum profile in the rest frame. In other words  $S_i \propto s(\nu)$  for every object  $i$  in our survey, and  $s(\nu)$  any function.

#### 3.1. Monochromatic survey

First, we suppose that we are looking at a survey at a single wavelength  $\nu_o$ . At this wavelength, the spectral flux density  $S$  transforms as:

$$\begin{aligned} S_o(\nu_o) &= \delta(\boldsymbol{\theta}_o) S_r(\nu_o) \delta(\boldsymbol{\theta}_o)^{-1} \\ &\approx (1 + \boldsymbol{\beta} \cdot \boldsymbol{\theta}_o) \left( S_r(\nu_o) - \nu_o \frac{\partial S_r}{\partial \nu_o} \boldsymbol{\beta} \cdot \boldsymbol{\theta}_o \right). \end{aligned} \quad (13)$$

We obtain  $S_o(\boldsymbol{\theta}_o, \nu_o) = S_r(\nu_o) + \delta S(\boldsymbol{\theta}_o, \nu_o)$ , where  $\delta S(\boldsymbol{\theta}_o, \nu_o)$  is defined as:

$$\begin{aligned} \delta S(\boldsymbol{\theta}_o, \nu_r) &\approx \left( S_r(\nu_o) - \nu_o \frac{\partial S_r}{\partial \nu_o} \right) \boldsymbol{\beta} \cdot \boldsymbol{\theta}_o \\ &\approx S(\nu) \left( 1 - \frac{\partial \log S}{\partial \log \nu} \right) \boldsymbol{\beta} \cdot \boldsymbol{\theta}_o. \end{aligned} \quad (14)$$

Note that here, every quantity in the rest frame can be expressed in the observer frame since the difference is in  $\mathcal{O}(\beta)$ , and becomes  $\mathcal{O}(\beta^2)$  after multiplication by  $\boldsymbol{\beta} \cdot \boldsymbol{\theta}_o$ . Therefore, for the sake of simplicity in the following we will drop the indices indicating the frame for every term proportional to  $\boldsymbol{\beta}$ . The number count becomes:

$$\begin{aligned} N_{\Omega, o}(> S_{\text{lim}}, \boldsymbol{\theta}_o) &= \delta(\boldsymbol{\theta}_o)^2 N_{\Omega, r}(> S_{\text{lim}} - \delta S_{\text{lim}}, \boldsymbol{\theta}_r) \\ &\approx (1 + 2\boldsymbol{\beta} \cdot \boldsymbol{\theta}_o) \left( \bar{N}_\Omega(> S_{\text{lim}}) - \frac{\partial \bar{N}_\Omega}{\partial S_{\text{lim}}} \delta S_{\text{lim}} \right) \\ &\approx \bar{N}_\Omega \left( 1 + \left( 2 - \frac{\partial \log N}{\partial \log S_{\text{lim}}} \left( 1 - \frac{\partial \log S}{\partial \log \nu} \right) \right) \boldsymbol{\beta} \cdot \boldsymbol{\theta}_o \right). \end{aligned} \quad (15)$$

As before, in the rest frame,  $N_{\Omega, r}(> S_{\text{lim}, r}, \boldsymbol{\theta}_r) = N(> S_{\text{lim}})/4\pi$ , and the kinematic dipole in the observer frame is:

$$D_{\text{kin}} = \left( 2 - \frac{\partial \log N}{\partial \log S_{\text{lim}}} \left( 1 - \frac{\partial \log S}{\partial \log \nu} \right) \right) \boldsymbol{\beta}. \quad (16)$$

This expression is strictly equivalent to the EB formula (12), where we took effective coefficient:

$$x_{\text{eff}} = -\frac{\partial \log N}{\partial \log S_{\text{lim}}} \quad (17)$$

at the limiting flux density  $S_{\text{lim}}$ . This is expected since only the objects with a flux density close to the limit appear or disappear from the number count with Doppler boosting.

$$\alpha_{\text{eff}} = -\frac{\partial \log S}{\partial \log \nu} \quad (18)$$

at the frequency  $\nu_o$ . In particular, it is notable that when the observed wavelength is close to a strong emission line, and every source have the same redshift, this  $\alpha_{\text{eff}}$  could become huge, in the negative or positive depending on the position of this emission line with  $\nu_o$ . This could lead to a sudden jump in the number count dipole. However, an important property of the spectral index is lost in this general case, it is no longer redshift independent. If we take into account that the spectra of every sources get shifted according to their individual redshift  $S_i(\nu) \rightarrow S_i((1 + z_i)\nu)$ , the  $\alpha_{\text{eff}}$  also gets modified. However, this doesn't affect the power law, as the redshift doesn't impact the spectrum profile, and it stays a power law.

#### 3.2. Photometric survey

In practice, cosmological surveys often don't scan the sky at a monochromatic frequency  $\nu_o$ , but give the luminosity (or equivalently, the magnitude) of every objects in a given band  $X$ . This luminosity can be expressed using the transmission function of the filter  $f_X(\nu)$ , here in terms of received energy:

$$L = \int d\nu f_X(\nu) S(\nu), \quad (19)$$

Note that here we neglected the transmission function of the atmosphere itself for ground based telescope, but the effect of atmosphere can be included in this filter transmission function. Suppose that we are looking at a particular object in the direction  $\boldsymbol{\theta}_o$  whose spectral flux density is  $S_o(\nu_o)$ , its luminosity transforms in the observer frame as:

$$\begin{aligned} L_o(\boldsymbol{\theta}_o) &= \int d\nu_o f_X(\nu_o) S_o(\nu_o) \\ &= \delta(\boldsymbol{\theta}_o)^2 \int d\nu_r f_X(\delta(\boldsymbol{\theta}_o)\nu_r) S_r(\nu_r) \\ &\approx (1 + 2\boldsymbol{\beta} \cdot \boldsymbol{\theta}_o) \int d\nu_r \left( f_X(\nu_r) + \boldsymbol{\beta} \cdot \boldsymbol{\theta}_o \nu_r \frac{\partial f_X}{\partial \nu_r} \right) S_r(\nu_r). \end{aligned} \quad (20)$$

We obtain  $L_o(\boldsymbol{\theta}_o) = L_r + \delta L(\boldsymbol{\theta}_o)$ , where  $\delta L(\boldsymbol{\theta}_o)$  is defined as:

$$\begin{aligned} \delta L(\boldsymbol{\theta}_o) &\approx \left( 2L + \int d\nu \nu \frac{\partial f_X}{\partial \nu} S(\nu) \right) \boldsymbol{\beta} \cdot \boldsymbol{\theta}_o \\ &\approx \left( L - \int d\nu f_X(\nu) \nu \frac{\partial S}{\partial \nu} \right) \boldsymbol{\beta} \cdot \boldsymbol{\theta}_o. \end{aligned} \quad (21)$$

Note that we used  $f_X(\nu) = f'_X(\nu) = 0$  outside of a particular frequency interval. For the same reason as  $\delta S$  in the monochromatic survey, every quantity here can be expressed either in the rest frame or in the observer frame.

The number count becomes:

$$\begin{aligned}
 N_{\Omega,o}(>L_{\lim}, \theta_o) &= \delta(\theta_o)^2 N_{\Omega,r}(>L_{\lim} - \delta L_{\lim}, \theta_r) \\
 &\approx (1 + 2\beta \cdot \theta_o) \left( \bar{N}_\Omega(>L_{\lim}) - \frac{\partial \bar{N}_\Omega}{\partial L_{\lim}} \delta L_{\lim} \right) \\
 &\approx \bar{N}_\Omega + \\
 &\bar{N}_\Omega \left( 2 - \frac{\partial \log N}{\partial \log L_{\lim}} \left( 1 - \frac{\int d\nu f_X(\nu) \nu \frac{\partial S_{\lim}}{\partial \nu}}{L_{\lim}} \right) \right) \beta \cdot \theta_o,
 \end{aligned} \tag{22}$$

where  $S_{\lim}(\nu)$  here is such as that its integrated luminosity is  $L_{\lim} = \int d\nu f_X(\nu) S_{\lim}(\nu)$ . As before, we can define effective coefficient  $x_{\text{eff}}$  and  $\alpha_{\text{eff}}$  where:

$$x_{\text{eff}} = -\frac{\partial \log N}{\partial \log L_{\lim}} = +2.5 \frac{\Phi(m_{\lim})}{N}, \tag{23}$$

with  $\Phi(m) = \frac{dN}{dm}$  the luminosity function of the survey,  $m_{\lim}$  the magnitude corresponding to  $L_{\lim}$ , and:

$$\alpha_{\text{eff}} = -\frac{\int d\nu f_X(\nu) \nu \frac{\partial S}{\partial \nu}}{\int d\nu f_X(\nu) S(\nu)} = 1 + \frac{\int d\nu \frac{\partial f_X(\nu)}{\partial \nu} \nu S(\nu)}{\int d\nu f_X(\nu) S(\nu)}. \tag{24}$$

Note that with  $f_X(\nu) = \nu_o \delta(\nu - \nu_o)$  for a given wavelength  $\nu_o$ , we obtain the same coefficients as for the monochromatic survey, which is expected. If we also suppose that  $S \propto s(\nu) = \nu^{-\alpha}$ , we have  $\alpha_{\text{eff}} = \alpha$ , whatever be the filter  $f_X(\nu)$ . We have shown that the EB formula (12) is still valid for any spectrum profile and luminosity function, provided that the  $x$  and  $\alpha$  coefficient are defined with more precision. However, as before we lost the property of the redshift independence of the spectral index.

#### 4. Effective spectral index for quasars

Now that we have an expression for the general effective coefficient for any spectral profile, we want to apply this new expression of  $\alpha_{\text{eff}}$  to real data. In particular, we want to see if the method to obtain  $\alpha$  coefficient used in (Secrest et al. 2021), which we will denote  $\alpha_{\text{mag}}$  in the following, yields the same results as this one. Using the W1 and W2 bands of the CatWISE survey, this method compares the difference of magnitude W1-W2, with a table of the same quantity calculated for synthetic pure-power law spectra with different  $\alpha$  coefficient.

To obtain  $\alpha_{\text{eff}}$  coefficients, we need quasar spectra in this W1 band, which expands from 2.7 to 3.9  $\mu\text{m}$  (Eisenhardt et al. 2020). We will use the AKARI QSONG catalog (Myungshin et al. 2017), which is a compilation of 753 quasars' spectra taken between 2.5 and 5  $\mu\text{m}$ . However, since we want a good spectral quality, we will only keep the spectra with a mean spectral flux density above 5 mJy and a positive value for  $\alpha_{\text{fit}}$ , which brings 41 individual quasars, and we can then extract their corresponding W1 and W2 band magnitude from the CatWISE2020 catalog (Marocco et al. 2021). We also use the transmission filter  $f_{\text{W1}}(\nu)$ , given by CatWISE<sup>1</sup>.

Now, we can apply equation (24) to these spectra to obtain the effective spectral index  $\alpha_{\text{eff}}$ . We will use the Python

package uncertainty to estimate the error bars<sup>2</sup>. It has to be noted that a *naive* integration of (24) can lead to huge error bars in the result: the gradient of the spectra is often smaller than its uncertainty here; however the gradient is not a set of independent variables, it is constrained by the value of the sum of it. Error propagation must be carefully handled, and it may be better suited to use the last term of the expression (24) which doesn't involve this gradient. Then, we can infer the corresponding spectral index  $\alpha_{\text{mag}}$ , with the CatWISE magnitude. Lastly, we will also fit the spectra within the range of the W1 band with a power law to obtain a last spectral index  $\alpha_{\text{fit}}$ .

We compare the different spectral indices obtained with these three methods in Fig. 2. We can see that the uncertainty in calculating  $\alpha_{\text{eff}}$  is quite large, which is explained by the large uncertainty of the spectra themselves. It is notable that the two point with the biggest deviation between this  $\alpha_{\text{eff}}$  and the other two methods correspond to the two spectra with the lowest spectral flux density. This emphasize the necessity to have a good spectral quality to calculate  $\alpha_{\text{eff}}$  precisely. For all of these quasars, we obtain:

$$\begin{aligned}
 \langle \alpha_{\text{eff}} - \alpha_{\text{fit}} \rangle &= -0.01 \quad \sigma = 0.33, \\
 \langle \alpha_{\text{eff}} - \alpha_{\text{mag}} \rangle &= 0.15 \quad \sigma = 0.42, \\
 \langle \alpha_{\text{fit}} - \alpha_{\text{mag}} \rangle &= 0.16 \quad \sigma = 0.22,
 \end{aligned}$$

We lack the statistical significance to make any definitive claim, however nothing leads us to think that these three methods yields significantly different results for quasars. At most, it seems that the  $\alpha_{\text{mag}}$  are slightly smaller than the other spectral indexes. If we consider that this method overestimate by 0.16 the  $\alpha$ , and with a mean measured value for the quasars in (Secrest et al. 2021) for  $\alpha$  being 1.26, the quantity  $2 + x(1 + \alpha)$ , with  $x = 1.89$ , would be at most underestimated by about 4%. This discrepancy might be explained by a slight difference in slope between the W1 and W2 band, but further investigation would be necessary to obtain conclusive evidences. Lastly, an example of a quasar spectrum taken from AKARI with its corresponding  $\alpha_{\text{eff}}$  and  $\alpha_{\text{mag}}$  is shown in Fig. 3.

#### 5. Conclusion

In this letter, we have demonstrated that the Ellis & Baldwin formula can be generalized to any class of light sources, regardless of their spectral shape or luminosity distribution, provided the coefficients  $x$  and  $\alpha$  are appropriately redefined. This result is essential for addressing the cosmic dipole anomaly, as it shows that sources other than quasars and radio galaxies can, in principle, be used to measure our velocity relative to the CRF.

We have also shown that, in the case of quasars, using spectra from AKARI, the resulting effective coefficient  $\alpha$  within the CatWISE W1 band is generally consistent with the value obtained by fitting the spectrum with a pure power law. Moreover, we find that the procedure used in (Secrest et al. 2021), which relies only on the W1 and W2 magnitudes, may slightly underestimate the true spectral index by up to  $\sim 0.16$ . Still, this difference is not sufficient to significantly alter the conclusions of this work, that has shown that the quasar dipole is a factor of  $\sim 2$  larger than the kinematic dipole expectation. Nevertheless, the limited

<sup>1</sup> The transmission in response per photon is given here <https://www.astro.ucla.edu/~wright/WISE/passbands.html>

<sup>2</sup> See <https://pythonhosted.org/uncertainties/>

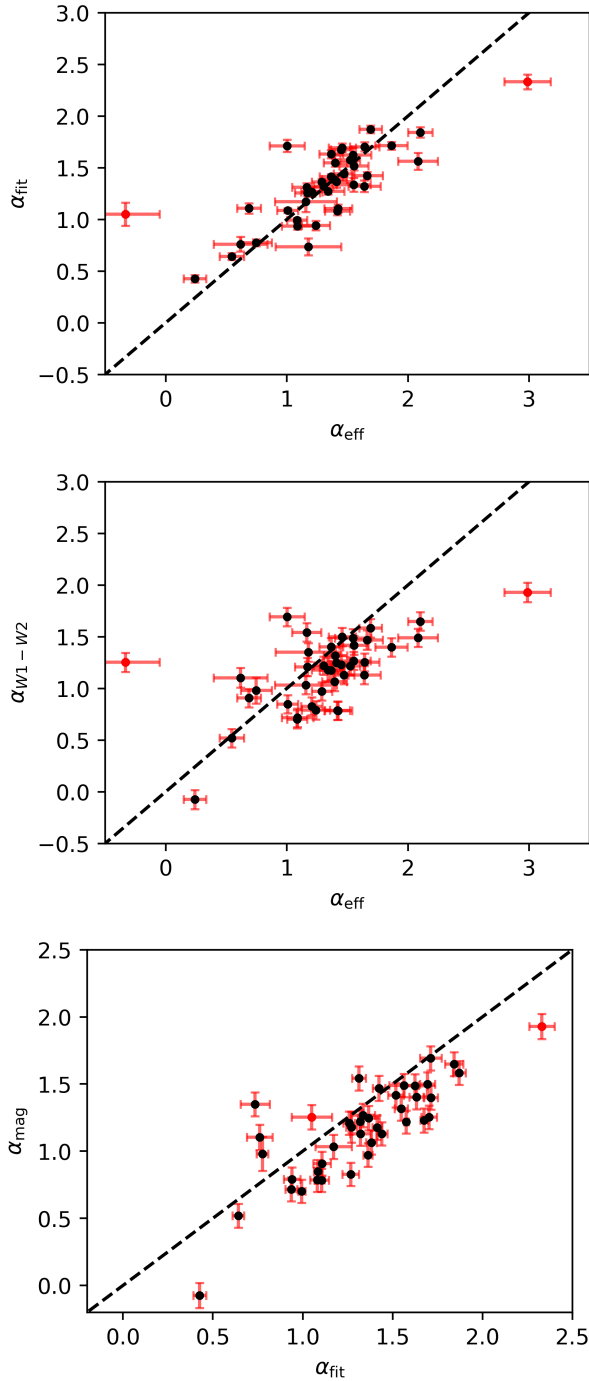


Fig. 2: Comparison of the spectral index  $\alpha$  obtained with different methods, for 41 quasar's spectra. The black dashed line corresponds to the identity. The two red dots with a high deviation between their calculated  $\alpha_{\text{eff}}$  and the two other method corresponds to the two quasars with the lowest mean spectral flux density.

number of available quasar spectra in this band prevents us from drawing definitive conclusions on this point. In the future, this issue may be clarified using spectroscopic libraries from missions such as SPHEREx (Crill et al. 2020).

In the general case, however, determining these new effective coefficients rigorously for a given dataset remains challenging, particularly for the effective spectral index  $\alpha_{\text{eff}}$ .

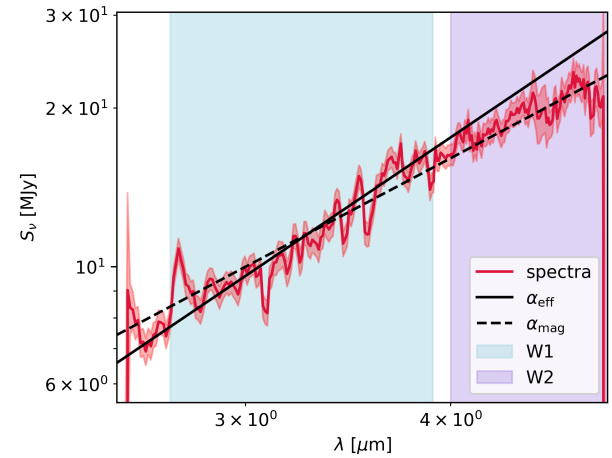


Fig. 3: Example of a spectrum for a quasar (PG2112+059, located at  $(272.101907, 64.128918)$ , in galactic coordinates) given by AKARI, with the spectral indexes  $\alpha_{\text{mag}}$  obtained using the  $W1 - W2$  method, and  $\alpha_{\text{eff}}$  using a direct integration of the spectra using (24). These spectral indexes are plotted as pure power laws  $S_{\nu} \propto \nu^{-\alpha}$ .

First, the spectral index is no longer independent of redshift. This is not necessarily problematic, as (von Hausegger 2024) showed that the original EB formula remains valid even when the indexes varies with redshift,  $\alpha(z)$  and  $x(z)$ , provided some redefinitions. However, if this demonstration can be adapted to this general case of non-power laws is still an open question. Beyond this, another important issue is that most wide-area sky surveys are photometric, and the calculation of  $\alpha_{\text{eff}}$  requires a good quality of spectra within the range of the photometric band, and spectra are typically available for only a small subset of objects through cross-matching. This may introduce biases which will have to be carefully handled. Future applications of this test will need to address these issues directly.

*Acknowledgements.* The author thanks Roya Mohayae, Nathan Secrest, Reza Ansari, Johann Cohen-Tanugi and Reiko Nakajima for their important insights and help.

## References

- Abghari, A., Bunn, E. F., Hergt, L. T., et al. 2024, Journal of Cosmology and Astroparticle Physics, 2024, 067
- Burles, S. & Rappaport, S. 2006, The Astrophysical Journal, 641, L1
- Collaboration, P., Aghanim, N., Akrami, Y., et al. 2020, Astronomy & Astrophysics, 641, A6
- Crill, B. P., Werner, M., Akeson, R., et al. 2020, in Space Telescopes and Instrumentation 2020: Optical, Infrared, and Millimeter Wave, 10
- Dalang, C. & Bonvin, C. 2022, Monthly Notices of the Royal Astronomical Society, 512, 3895
- Eisenhardt, P. R. M., Marocco, F., Fowler, J. W., et al. 2020, The Astrophysical Journal Supplement Series, 247
- Ellis, G. F. R. & Baldwin, J. E. 1984, Monthly Notices of the Royal Astronomical Society, 206, 377
- Euclid Collaboration, Mellier, Y., Abdurro'uf, et al. 2025, *äp*, 697, A1
- Gibelyou, C. & Huterer, D. 2012, Monthly Notices of the Royal Astronomical Society, 427, 1994
- Ivezic, Z., Kahn, S. M., Tyson, J. A., et al. 2019, *\textbackslash textbackslash apj*, 873, 111
- Maartens, R., Clarkson, C., & Chen, S. 2018, Journal of Cosmology and Astroparticle Physics, 2018, 013
- Marocco, F., Eisenhardt, P. R. M., Fowler, J. W., et al. 2021, The Astrophysical Journal Supplement Series, 253, 8

Moriconi, M. 2006, European Journal of Physics, 27, 1409

Myungshin, I., Hyungsung, J., Dohyeong, K., et al. 2017, Publications of The Korean Astronomical Society, 32, 163

Nadolny, T., Durrer, R., Kunz, M., & Padmanabhan, H. 2021, Journal of Cosmology and Astroparticle Physics, 2021, 009

Secrest, N., Hausegger, S. v., Rameez, M., Mohayaee, R., & Sarkar, S. 2022, The Astrophysical Journal Letters, 937, L31

Secrest, N., Hausegger, S. v., Rameez, M., et al. 2021, The Astrophysical Journal Letters, 908, L51

Secrest, N., von Hausegger, S., Rameez, M., Mohayaee, R., & Sarkar, S. 2025, Reviews of Modern Physics, 97, 041001

von Hausegger, S. 2024, Monthly Notices of the Royal Astronomical Society: Letters, 535, L49

von Hausegger, S., Secrest, N., Desmond, H., et al. 2025, Clustering properties of the CatWISE2020 quasar catalogue and their impact on the cosmic dipole anomaly